Received: 3 August 2023 | Revised: 16 October 2023 | Accepted: 19 October 2023

DOI: 10.1111/acel.14033

Aging Cell WILEY

RESEARCH ARTICLE

Genetic context drives age-related disparities in synaptic maintenance and structure across cortical and hippocampal neuronal circuits

Sarah E. Heuer[1,2] | Emily W. Nickerson[1,2] | Gareth R. Howell[1,2,3] | Erik B. Bloss[1,2,3]

[1]The Jackson Laboratory, Bar Harbor, Maine, USA

[2]Tufts University Graduate School of Biomedical Sciences, Boston, Massachusetts, USA

[3]Graduate School of Biomedical Sciences and Engineering, University of Maine, Orono, Maine, USA

Correspondence
Gareth R. Howell and Erik B. Bloss, The Jackson Laboratory, Bar Harbor, ME 04609, USA.
Email: erik.bloss@jax.org and gareth.howell@jax.org

Funding information
National Institute on Aging, Grant/Award Number: AG055104, AG062409 and AG079877

Abstract

The disconnection of neuronal circuitry through synaptic loss is presumed to be a major driver of age-related cognitive decline. Age-related cognitive decline is heterogeneous, yet whether genetic mechanisms differentiate successful from unsuccessful cognitive decline through maintenance or vulnerability of synaptic connections remains unknown. Previous work using rodent and primate models leveraged various techniques to imply that age-related synaptic loss is widespread on pyramidal cells in prefrontal cortex (PFC) circuits but absent on those in area CA1 of the hippocampus. Here, we examined the effect of aging on synapses on projection neurons forming a hippocampal-cortico-thalamic circuit important for spatial working memory tasks from two genetically distinct mouse strains that exhibit susceptibility (C57BL/6J) or resistance (PWK/PhJ) to cognitive decline during aging. Across both strains, synapse density on CA1-to-PFC projection neurons appeared completely intact with age. In contrast, we found synapse loss on PFC-to-nucleus reuniens (RE) projection neurons from aged C57BL/6J but not PWK/PhJ mice. Moreover, synapses from aged PWK/PhJ mice but not from C57BL/6J exhibited altered morphologies that suggest increased efficiency to drive depolarization in the parent dendrite. Our findings suggest resistance to age-related cognitive decline results in part by age-related synaptic adaptations, and identification of these mechanisms in PWK/PhJ mice could uncover new therapeutic targets for promoting successful cognitive aging and extending human health span.

KEYWORDS
aging, frontal cortex, genetic diversity, neuronal circuits, synaptic plasticity

Abbreviations: A, aged; AAV, adenoassociated virus; AD, Alzheimer's disease; ANOVA, analysis of variance; B6, C57BL/6J mouse strain; CA1, hippocampal area CA1; CA1-to-PFC, neuronal circuit projecting from hippocampal CA1 to the prefrontal cortex; CA3, hippocampal area CA3; EC, entorhinal cortex; EGFP, expression green fluorescent protein; K-S, Kolmogorov-Smirnov; M, middle-aged; MA, middle-aged versus aged; NHP, non-human primate; PFC, prefrontal cortex; PFC-to-RE, neuronal circuit projecting from the prefrontal corext to the nucleus reuniens; PWK, PWK/PhJ mouse strain; Q1, quartile 1; Q4, quartile 4; RE, nucleus reuniens; SNP, single nucleotide polymorphism; tdTomato, tandem dimer Tomato; Y, young; YA, young versus aged; YM, young versus middle-aged.

1 | INTRODUCTION

Synapses are the fundamental computational subunits of the brain, and the building blocks of neuronal circuits that vary in complexity based on brain region and mammalian organism (Lerner et al., 2016; Südhof & Malenka, 2008). Synapses enable cell-type specific forms of communication and are often targeted to defined spatial subcellular locations on postsynaptic cell types, which constrains neural circuit operations (Bloss et al., 2016, 2018; Brown & Hestrin, 2009; Druckmann et al., 2014; Gidon & Segev, 2012; Katz et al., 2009; Koch et al., 1983). Synapses act as plastic, tunable biochemical and electrical signaling compartments, a feature that allows internal states to shape neural circuit function (Matsuzaki et al., 2004; Turrigiano, 2008), and may be the primary substrate in the nervous system mediating learning and memory recall (Harvey & Svoboda, 2007; Kasai et al., 2003).

Individual excitatory synapses on many neuronal cell types take the form of small protrusions along the dendrites (i.e., dendritic spines (Cajal, 1888)), which can be visualized by multiple imaging methods (Kasai et al., 2003; Matsuzaki et al., 2001; Serrano et al., 2022). Spine structure reflects the functional strength of each connection: spine head size correlates with synapse strength (Kasai et al., 2003; Matsuzaki et al., 2001), and the morphology of the spine neck determines the degree of electrical and biochemical filtering that occurs between the synapse and the parent dendritic cable (Grunditz et al., 2008; Tønnesen et al., 2014). During normal aging, mammalian organisms experience progressive, yet variable, cognitive decline, even in the absence of a disease, which corresponds to a loss in synaptic plasticity (Burke & Barnes, 2006). Relative to other synapses, spine synapses seem to be the primary type that are lost or altered during aging, and these changes in the aging brain appear circuit specific (Dickstein et al., 2013; Morrison & Baxter, 2012). For example, the density of spine synapses decreases over time on cortical neurons in the frontal but not visual cortex, and decreases on CA3 pyramidal neurons but not on neighboring neurons in CA1 (Fan et al., 2017; Morrison & Baxter, 2012; Young et al., 2014). The loss of synapse number and the changes in synaptic structure on frontal cortical neurons correlate with progressive reductions in cognitive function with age (Brennan et al., 2009; Hara et al., 2012; Luebke et al., 2004), yet reports of the degree to which synaptic loss occurs suggests significant heterogeneity (Bloss et al., 2011; Morrison & Baxter, 2012; Scheff et al., 1991, 2001). The causal factors that underlie this variability could be what determines successful versus unsuccessful neural aging (Morrison & Baxter, 2012; Morrison & Hof, 1997; Moss et al., 2007), and there is significant interest in understanding how genetic components and environmental influences coordinately shape the trajectory of age-related cognitive changes and synaptic connectivity.

Non-human primates (NHPs) (Hof & Morrison, 2004; Luebke et al., 2004; Peters et al., 2008) and rodents (rats (Barnes & McNaughton, 1985; Bloss et al., 2011; Bloss et al., 2013) and mice (Cizeron et al., 2020)) are commonly used model systems to study the effect of aging on synapses. Although NHPs are the most translatable model for relating age-related neural circuit changes to cognitive decline (Dumitriu et al., 2010; Luebke et al., 2004), they have long lifespans (>30 years), require complex housing systems, and are not amendable to genetic-based experimentation at scale. Data from rodent models recapitulate the magnitude of age-related synaptic loss in vulnerable brain regions (including the prefrontal cortex) that has been observed in NHPs (Bloss et al., 2011; Rasmussen et al., 1996; Scheff et al., 1991). Studies in mice have shown loss in synaptic plasticity and number during aging and in age-related diseases (Jacobsen et al., 2006; Neuman et al., 2015; Nicholson et al., 2004). Unlike NHP experiments, which necessarily use genetically diverse non-inbred subjects, the work in mice has largely been performed using the inbred C57BL/6J (B6) mouse strain. This lack of genetic diversity limits translatability of mouse work to humans, and has led us to evaluate the potential of incorporating genetically distinct wild-derived inbred mouse strains in our own work (Keane et al., 2011). Our previous results show wild-derived strains exhibit diverse cognitive and behavioral phenotypes during aging and when carrying Alzheimer's disease (AD)-linked transgenes, suggesting genetic background may influence neuronal circuitry and function (Fernandes et al., 2004; Onos et al., 2019). In particular, the PWK/PhJ (PWK) mouse strain did not show amyloid-dependent cognitive decline or synaptic loss, suggesting PWK is an ideal strain to study resilience to AD (Heuer et al., 2023). However, the neuronal circuits vulnerable in aging are different than those vulnerable to AD, and it remains unknown whether PWK is also resistant to normal age-related synaptic loss.

To determine the effect of genetic context on age-related synapse dynamics (and how they might relate to their observed cognitive susceptibility/resilience (Gregorová & Forejt, 2000; Onos et al., 2019)), we examined aging-related synapse loss in the traditionally studied B6 and wild-derived PWK mouse strains. PWK mice differ from B6 by approximately 20 million single nucleotide polymorphisms (SNPs) and structural variants (Keane et al., 2011). To target our analyses to specific projection neurons, we leveraged retrograde viral strategies to label two circuits known to have different vulnerabilities to aging or AD: PFC-projecting neurons to nucleus reuniens (RE; PFC-to-RE), and CA1-projecting neurons to PFC (CA1-to-PFC) (Dickstein et al., 2013). We show that spine synapses on CA1-to-PFC neurons showed marked stability throughout aging in both B6 and PWK mice. In contrast, PFC-to-RE neurons were susceptible to age-related spine loss in B6 but not PWK. Further, there were morphological changes suggestive of synapse strengthening in PWK but not B6 mice. Collectively, these results provide evidence that PWK are a model of successful synaptic aging.

2 | RESULTS

2.1 | Labelling strategies to visualize synapses from two neural circuits in genetically distinct mice

Our previous studies suggest PWK mice are a model of cognitive, neuronal and synaptic resilience to Aβ pathology (Heuer et al., 2023; Onos et al., 2019). However, since age is the leading risk factor for developing AD, we tested the prediction that PWK would also be a

model of successful synaptic aging when compared to traditionally used inbred B6 mice. We leveraged previously established viral approaches (Graham et al., 2021; Tervo et al., 2016) using two different reporter fluorophores to visualize excitatory projection neurons forming two arms of a connected hippocampal-cortico-thalamic loop important for spatial working memory tasks (Ito et al., 2015). To remain consistent with previous work identifying female susceptibility to age-related diseases of the brain (Bailey et al., 2011; Baxter et al., 2018; Heuer et al., 2023; Onos et al., 2019; Yang et al., 2021), we chose to analyze female mice of both strains. Each set of projection neurons expressed either Expression Green Fluorescent Protein (EGFP) or tandem dimer Tomato (tdTomato) across cohorts of female B6 and PWK mice ranging from 4 to 29 months of age (Table S1). Three unilateral intracranial injection sites were targeted to deliver recombinant adenoassociated virus (AAV, see Methods) to drive EGFP in PFC neurons that project to RE (PFC-to-RE) and tdTomato expression in CA1 neurons that project to PFC (CA1-to-PFC). After 3–4 weeks, allowing for proper retrograde movement and fluorophore expression, each mouse was perfused, coronal slices were made with a vibratome, slices containing EGFP+ or tdTomato+ neurons were imaged, and dendritic spine density and morphologies were analyzed (Figure 1a). Three age groups were assessed: young (4–7 months of age), middle-aged (11–17 months of age), and aged (22–30 months of age) groups. Neurons making up the two projection circuits in B6 and PWK mice were labeled with equivalent efficiency, suggesting a similar overall density of neurons comprising these pathways from the compared strains (Figure 1b,c).

2.2 | Aging spines on proximal CA1 dendrites exhibit stable densities but altered morphologies in PWK but not B6 mice

The CA1 region of the hippocampus is well-studied on account of its anatomy, physiology, role in episodic memory, and vulnerability to both age- and AD-related pathological insults (Morrison & Hof, 1997). While generally thought to be relatively resistant to normal age-related synaptic loss (Buss et al., 2021; Geinisman et al., 2004; Nicholson et al., 2004), it is unclear if age-related structural changes occur on specific CA1 projections, and if they are modulated in subjects from genetic contexts that exhibit resistance to cognitive aging. The majority of excitatory inputs onto CA1 pyramidal cells are made onto the proximal apical oblique and basal branches (Bloss et al., 2018; Megías et al., 2001) which both receive inputs from hippocampal area CA3 (Empson & Heinemann, 1995). Therefore, we first analyzed dendritic spine synapses on branches from this proximal dendritic compartment

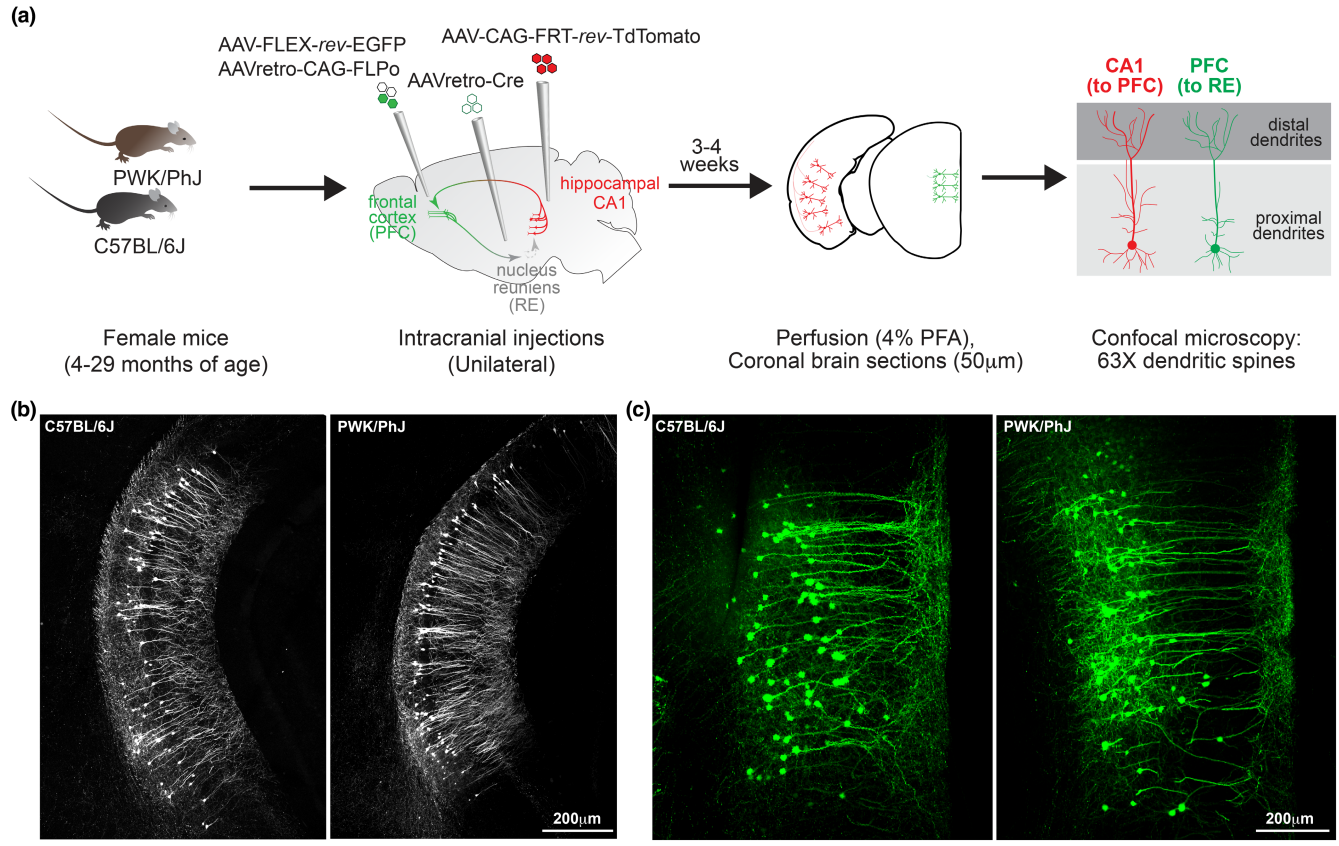

FIGURE 1 Viral labelling of PFC-to-RE and CA1-to-PFC neurons across C57BL/6J and PWK/PhJ mice. (a) Experimental outline (see *Methods* for additional details). (b, c) Example 10× images of tdTomato+ CA1 neurons (b) from B6 (left) and PWK (right) demonstrating consistent CA1-to-PFC projection circuit labelling, and EGFP+ PFC neurons (c) from B6 (left) and PWK (right) demonstrating consistent PFC-to-RE projection circuit labelling. Summary metadata for individual mice used in this study reported in Table S1.

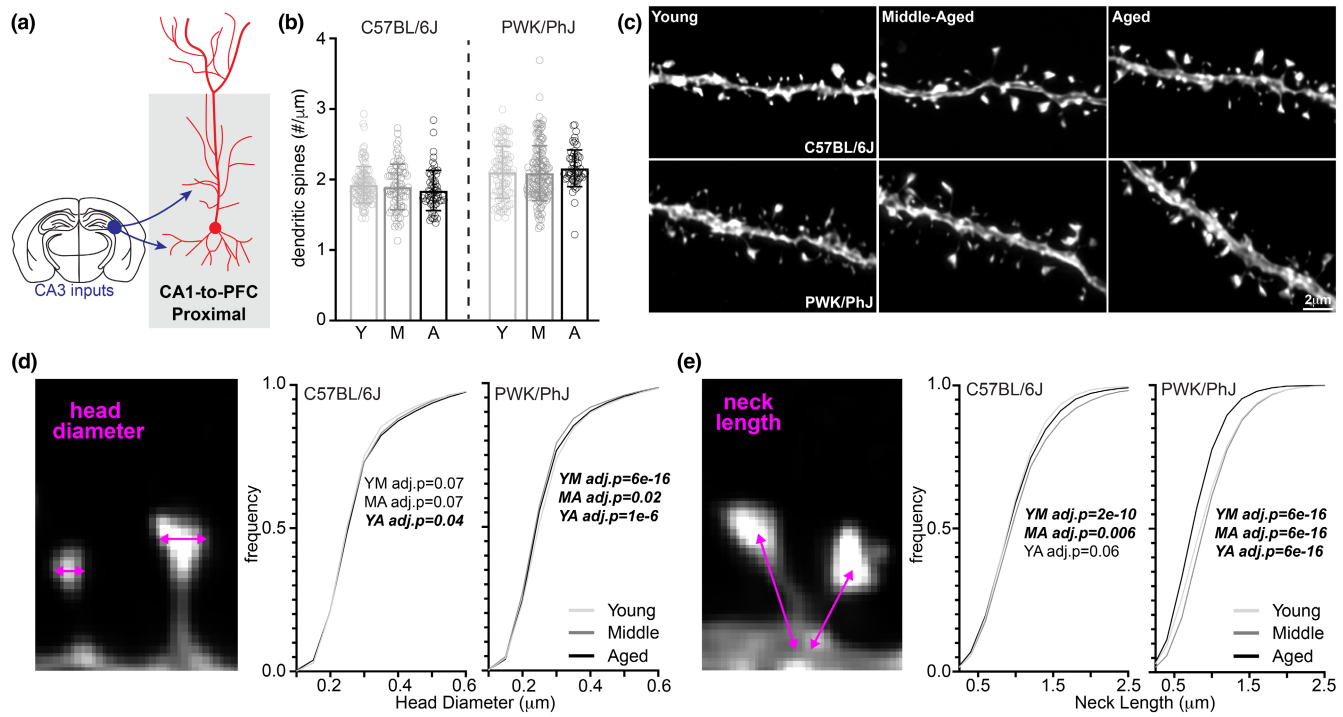

FIGURE 2 CA1-to-PFC proximal dendrites are resistant to synaptic density changes across both strains, but PWK/PhJ spines change morphologies. (a) Example schematic of tdTomato+ proximal CA1-to-PFC dendrites analyzed here and projection input origins in hippocampal area CA3. (b) Proximal CA1-to-PFC dendrite spine densities (spines/μm) comparing young (Y), middle-aged (M) and aged (A) within each strain. Data points represent individual branches ($n = 20$/mouse); error bars are ±SD; one-way ANOVA identified no significant effects within B6 or PWK (Table S2). (c) Representative 63× images of proximal CA1-to-PFC dendrites from each strain/age group. (d) CA1-to-PFC proximal spine head diameter example image (left) and cumulative distributions from B6 (middle) and PWK (right), across age groups. Kolmogorov–Smirnov tests were used to evaluate statistical significance (Bonferroni adjusted $p < 0.05$) of pairwise comparisons: young versus middle-aged (YM), middle-aged versus aged (MA), and young versus aged (YA), and *p*-values reported on each graph (see Table S2). Data points are representative of measures from individual spines. (e) Same as (d) for CA1-to-PFC proximal spine neck length. Summary statistics for data points represented in each graph reported in Table S2.

specifically on CA1-to-PFC neurons (Figure 2a). Consistent with the prediction from previous reports (Buss et al., 2021; Dickstein et al., 2013), we observed no significant age-related changes in proximal spine density in either B6 or PWK mice (Figure 2b,c).

Dendritic spines alter their morphologies in response to repeated artificial synaptic stimulation (Harvey & Svoboda, 2007; Matsuzaki et al., 2004), under conditions of homeostasis (Blanpied & Ehlers, 2004; Turrigiano, 2008), and in reaction to disease pathologies and during aging (Runge et al., 2020; Turrigiano, 2012). Spine head morphology is a reliable predictor of synaptic stability and strength (Kasai et al., 2003; Matsuzaki et al., 2001), so we analyzed the maximum head diameter of each reconstructed spine. Our analysis found no overt age-related changes in B6 mice, but the same analysis in PWK mice revealed a subtle yet significant age-related shift to spines with smaller head diameters (Figure 2d). This effect was evident when we examined the densities of spines across the smallest (Q1) and largest (Q4) quartiles of head diameters (Figure S1b).

The morphology of dendritic spine necks (e.g., neck width and length) are similarly plastic (Tønnesen et al., 2014) and define the compartmentalization of spines much more critically than spine head size (Araya et al., 2006; Grunditz et al., 2008; Sorra & Harris, 2000; Tønnesen et al., 2014). Dendritic spine necks act as strong electrical resistors, filtering currents from the synapse to the parent dendrite branch (Araya et al., 2006). Necks also contain receptors for neuromodulatory systems that regulate local excitability (Wang et al., 2007). Spine neck widths are often below 50 nm (Bloss et al., 2018) making them difficult to resolve with light microscopy. We analyzed putative spine neck lengths to determine whether this aspect of spine neck morphology is readily modified during aging. Neck lengths in B6 mice were slightly lengthened with age, complementing the stability observed in spine heads. In contrast, PWK spine neck lengths showed a biphasic response, first increasing from young to middle-aged, then decreasing significantly in aged mice compared to the younger groups (Figures 2e and S1c).

Classifying spines into morphological categories (or types) is a more traditional approach to characterizing synaptic morphology that encompasses changes to both spine head diameter and neck length (Ghani et al., 2017; Hering & Sheng, 2001). The four main spine types are long (>1 μm neck length), thin (0.3–1 μm neck length, <0.3 μm head diameter), mushroom (<1 μm neck length, >0.3 μm head diameter), and stubby spines (<0.3 μm neck length, <0.3 μm head diameter) (Risher et al., 2014). Many cross-species studies have found conflicting evidence towards changes to spine types with aging, suggesting that long, thin, mushroom and stubby spines

are affected differently depending on the brain region and neural circuit examined (Dickstein et al., 2013). We found strain-specific differences on changes to spine groups with age in CA1 pyramidal dendrites, with dendrites from B6 mice showing no significant differences and PWK exhibiting a significant reduction in long spines and increase in thin and mushroom spines with age (Figure S1d). These data support our findings that while spine populations from B6 CA1 pyramidal cells appear relatively static during aging, PWK spines undergo dynamic age-dependent morphological remodeling.

2.3 | Spine changes on distal CA1 dendrites mirror those found on proximal compartments

Distal tuft dendrites in CA1 pyramidal cells are thought to be the most vulnerable to AD-related synaptic changes due to their afferent inputs originating in the EC (Figure 3a) (Neuman et al., 2015), where associated neuropathology is observed very early in the disease process (Hampel et al., 2021; Kaufman et al., 2018). Synapses on distal dendrites are understudied relative to those on more proximal compartments due to limitations in traditional techniques used to evaluate plasticity at remote locations relative to the soma. Consistent with our results from the proximal dendrites, we observed no significant age-related changes to distal tuft spine densities in B6 or PWK mice (Figure 3b,c). Like spines from proximal branches, we observed few age-related changes in head diameter and neck length in spines from B6 distal branches (Figures 3d,e and S2b,c). However, spine head diameters were larger in aged PWK mice compared to young and middle-aged cohorts (Figures 3d and S2b), and spine neck lengths were significantly shorter in aged compared to young and middle-aged mice (Figures 3e and S2c). Changes to the proportion of spines belonging to morphological groups in distal CA1 pyramidal dendrites mirrored those observed in proximal dendrites, with B6 remaining relatively stable and PWK exhibiting a reduction in long spines and increase in thin and mushroom spines with aging (Figure S2d).

Collectively, these results show spine densities on proximal and distal dendrites from CA1-to-PFC pyramidal cells do not change with age in both B6 and PWK mice. Furthermore, B6 spines remained morphologically stable whereas PWK spines exhibited changes indicative of increased excitability at the synapse and to the parent dendritic cable, which support the notion that these adaptations could play a role in maintaining information processing in the aging hippocampus.

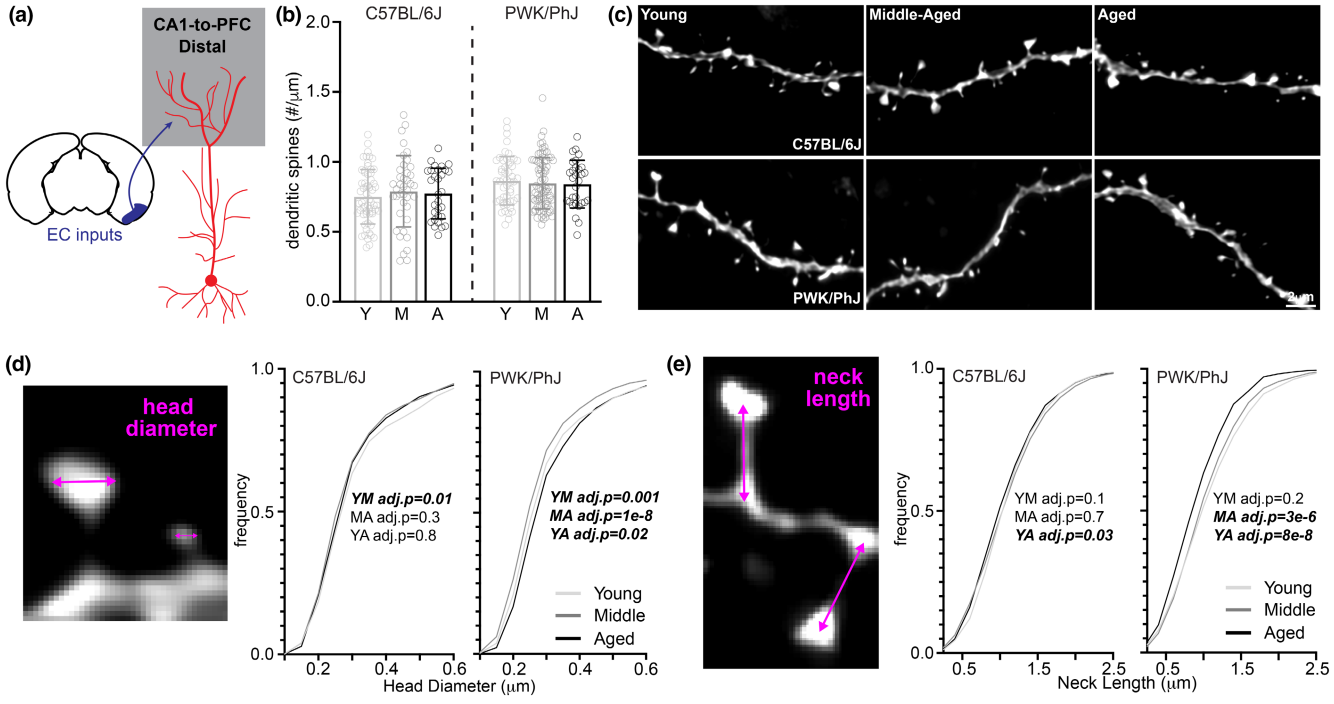

FIGURE 3 CA1-to-PFC distal tuft dendrites do not lose synapses but are morphologically altered in PWK/PhJ mice. (a) Example schematic of tdTomato+ distal tuft CA1-to-PFC dendrites analyzed here and projection input origins in entorhinal cortex (EC). (b) Distal tuft CA1-to-PFC dendrite spine densities (spines/μm) comparing young (Y), middle-aged (M) and aged (A) within each strain. Data points represent individual branches ($n = 10$/mouse); error bars are ±SD; one-way ANOVA identified no significant effects within B6 or PWK (Table S3). (c) Representative 63× images of distal tuft CA1-to-PFC dendrites from each strain/age group. (d) CA1-to-PFC distal tuft spine head diameter example image (left) and cumulative distributions from B6 (middle) and PWK (right), across age groups. Kolmogorov–Smirnov tests were used to evaluate statistical significance (Bonferroni adjusted $p < 0.05$) of pairwise comparisons: young versus middle-aged (YM), middle-aged versus aged (MA), and young versus aged (YA), and p-values reported on each graph (see Table S3). Data points are representative of measures from individual spines. (e) Same as (d) for CA1-to-PFC distal tuft spine neck length. Summary statistics for data points represented in each graph reported in Table S3.

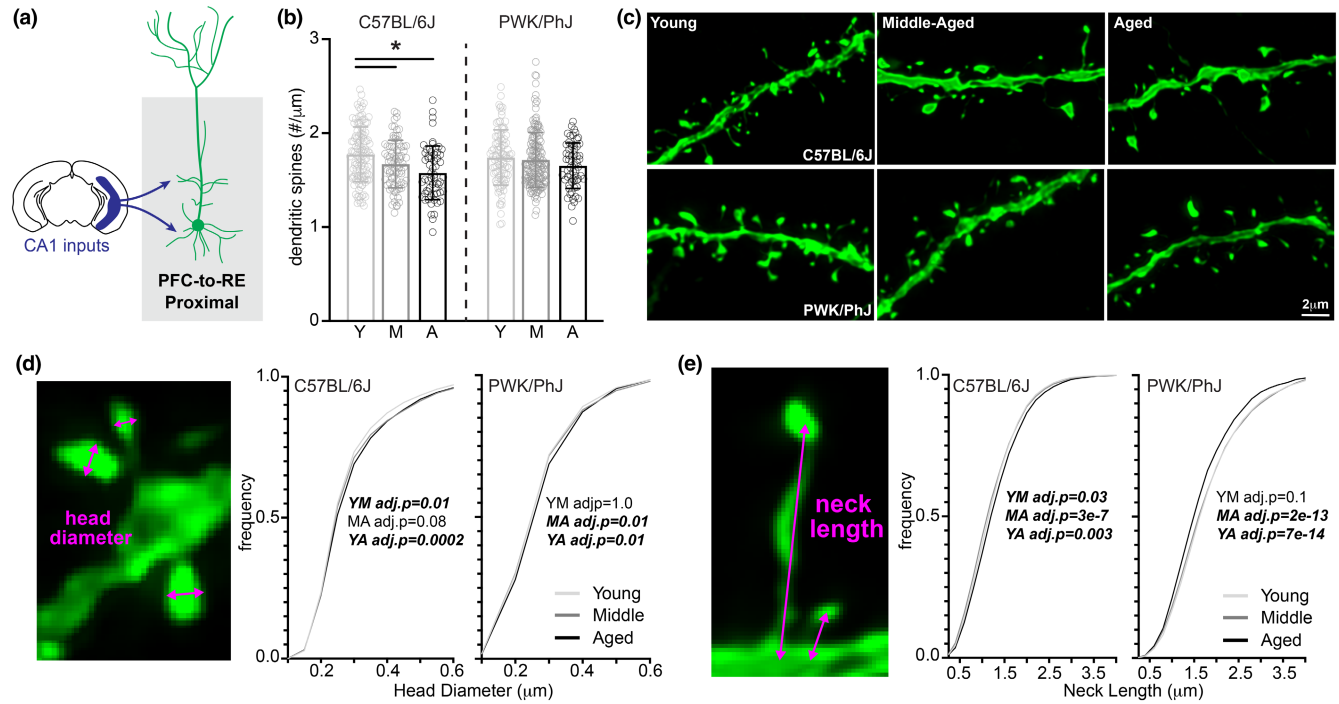

FIGURE 4 C57BL/6J mice are susceptible to age-related synaptic loss in proximal PFC-to-RE dendrites, with PWK/PhJ demonstrating dynamic morphological changes to increase synaptic strength. (a) Example schematic of EGFP+ proximal PFC-to-RE dendrites analyzed here and projection input origins in hippocampal area CA1. (b) Proximal PFC-to-RE dendrite spine densities (spines/μm) comparing young (Y), middle-aged (M) and aged (A) within each strain. Data points represent individual branches ($n = 20$/mouse); error bars are ±SD; one-way ANOVA identified significant effect within B6 but not PWK; asterisks denote significant (Bonferroni adjusted $p < 0.05$) comparisons identified using post hoc analysis within B6 (Table S4). (c) Representative 63× images of proximal PFC-to-RE dendrites from each strain/age group. (d) PFC-to-RE proximal spine head diameter example image (left) and cumulative distributions from B6 (middle) and PWK (right), across age groups. Kolmogorov–Smirnov tests were used to evaluate statistical significance (Bonferroni adjusted $p < 0.05$) of pairwise comparisons: young versus middle-aged (YM), middle-aged versus aged (MA), and young versus aged (YA), and p-values reported on each graph (see Table S4). Data points are representative of measures from individual spines. (e) Same as (d) for PFC-to-RE proximal spine neck length. Summary statistics for data points represented in each graph reported in Table S4.

2.4 | Differential vulnerability to age-related synaptic changes on PFC-to-RE neurons across B6 and PWK mice

Previous studies in humans, NHPs, rats and mice report that pyramidal neurons in the prefrontal cortex (PFC) are susceptible to synaptic loss with age (Bloss et al., 2011; Brennan et al., 2009; Luebke et al., 2004; Petanjek et al., 2011; Peters et al., 2008). Moreover, preventing this degeneration could be key to promoting successful cognitive aging (Brennan et al., 2009; Hao et al., 2007; Villeda et al., 2014). To test the prediction that PWK mice are resistant to age-dependent synaptic loss in the PFC, we used AAVs to label deep-layer neurons (in the same mice described above) in the PFC that project to the RE (Figure 1) that appear to mediate behavioral flexibility and working memory (Bayer & Bertoglio, 2020; Bizon et al., 2009; Kaczorowski et al., 2012). Like CA1-to-PFC neurons, PFC-to-RE neurons have an organized dendritic architecture, and the proximal and distal compartments each receive a distinct set of inputs. Basal and apical oblique dendrites located in the proximal regions receive afferent inputs from CA1 (among other regions), whereas distal tuft dendrites receive a distinct set of inputs from the thalamus (Graham et al., 2021) (Figure 4a). Therefore, we analyzed the spines on proximal and distal dendritic compartments separately.

We first examined spine density on proximal dendrites of PFC-to-RE neurons. Consistent with previous findings, B6 proximal dendritic spine density was significantly lower in middle-aged and aged compared to young mice (Shimada et al., 2003). Interestingly, we found no differences in spine densities on proximal PFC dendrites across age cohorts in PWK mice (Figure 4b,c). When we examined spine morphologies, we found statistically significant changes in spine head diameter with age on both B6 and PWK proximal PFC dendrites, evidenced by the cumulative frequency analyses and by quartile analysis of the largest and smallest spines (Figures 4d and S3b). In both B6 and PWK mice, PFC proximal spine head diameters became subtly larger with aging (Figure 4d). While spines on proximal dendrites from B6 mice showed minimal age-related changes in neck length, spines on proximal branches from PWK mice were significantly shortened with age. These changes that should reduce the degree to which the neck filters synaptic currents, mimic the patterns found on aging CA1 dendrites from PWK mice (Figures 4e and S3c). When classified into categories, spines from proximal PFC-to-RE dendrites in B6 mice showed a subtle but significant increase in

long spines with age, whereas PWK exhibited no significant changes in group composition with age (Figure S3d). These data suggest that the two neural circuits examined here have different strain-specific responses to aging in both spine density and morphology.

2.5 | Age-related dendritic spine loss and morphological remodeling on distal PFC dendrites differs between B6 and PWK mice

Distal tuft branches from PFC-to-RE projection neurons receive distinct afferent inputs compared to proximal branches, coming from the thalamus instead of CA1 (Graham et al., 2021) (Figure 5a). Like the age-related changes found on proximal dendrites of PFC-to-RE neurons, distal dendritic spine densities were lower in middle-aged and aged compared to young B6 mice but did not change across age groups in PWK mice (Figure 5b,c).

Spine head diameters on distal branches of PFC-to-RE neurons from B6 mice showed a biphasic response, first increasing in size between young and middle-aged cohorts, then decreasing in size between middle-aged to aged groups. PWK distal PFC spine heads displayed the opposite pattern: decreasing in size between young and middle-aged groups, and then increasing in size between middle-aged and aged cohorts (Figures 5d and S4b). Spine neck lengths on the distal dendrites of PFC-to-RE neurons from B6 mice slightly lengthened with age, while those from PWK decreased dramatically with age (Figure 5e). These changes in spine neck lengths were observed in quartile analyses, with a significant gain of long spine necks in aged B6 mice, and an overt loss of long spine necks in aged PWK mice (Figure S4c). Composition of spine types were also differentially altered with age, as spines from B6 distal PFC dendrites exhibited an increase in long and reduction of mushroom spines with age, whereas PWK were static (Figure S4d). These results from distal PFC-to-RE dendrites mirrored those from proximal dendrites: B6 branches showed age-related synaptic loss while those from PWK did not. In contrast, PWK distal PFC spines showed spine neck remodeling while those from B6 were markedly more stable, with PWK altering spine morphologies so that increased electrical signal is predicted to be driven to the spine (increase in large spines) and dendrite (reduction in spine necks).

Collectively, these data support our hypothesis that, like resilience to AD-related Aβ pathology (Onos et al., 2019), PWK mice show

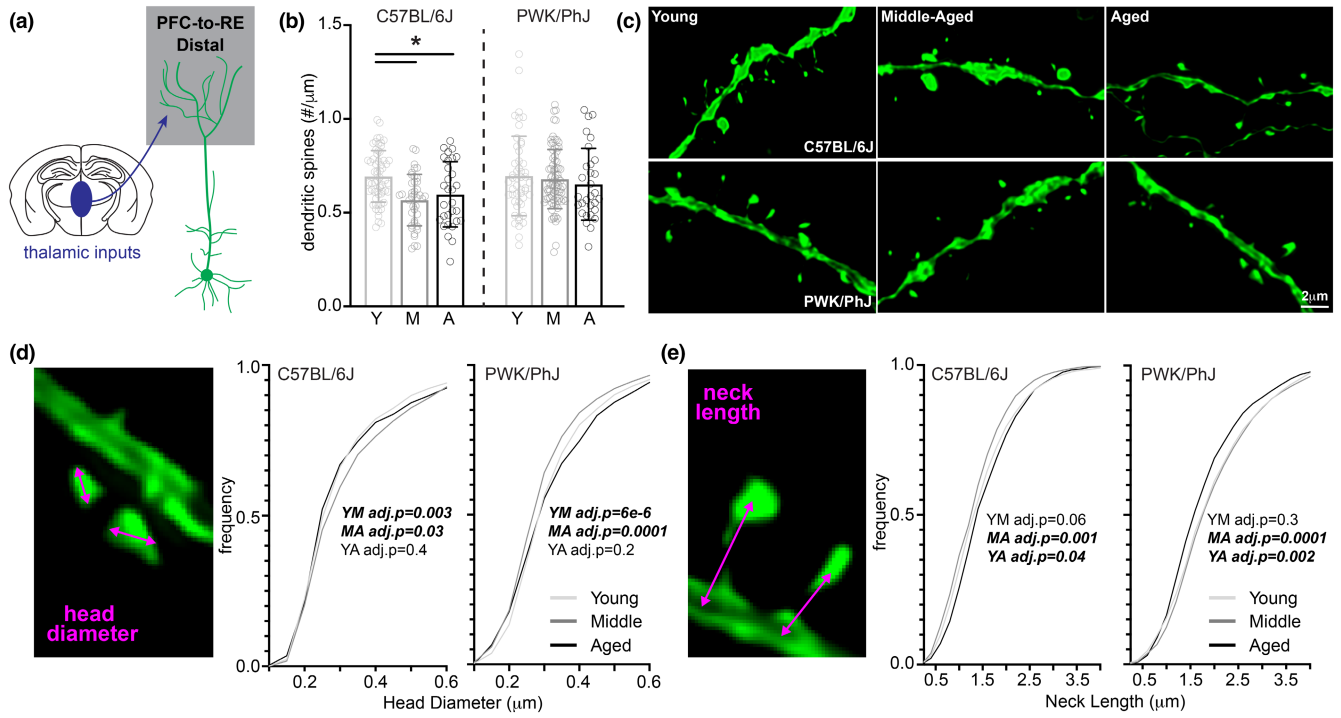

FIGURE 5 PFC-to-RE distal tuft dendrites exhibit age-induced synaptic loss in C57BL/6J mice but are morphology dynamic in PWK/PhJ mice. (a) Example schematic of EGFP+ distal tuft PFC-to-RE dendrites analyzed here and thalamic projection input origins. (b) Distal tuft PFC-to-RE dendrite spine densities (spines/μm) comparing young (Y), middle-aged (M) and aged (A) within each strain. Data points represent individual branches ($n = 10$/mouse); error bars are ±SD; one-way ANOVA identified significant effect within B6 but not PWK; asterisks denote significant (Bonferroni adjusted $p < 0.05$) comparisons identified using post hoc analysis within B6 (Table S5). (c) Representative 63× images of distal tuft PFC-to-RE dendrites from each strain/age group. (d) PFC-to-RE distal tuft spine head diameter example image (left) and cumulative distributions from B6 (middle) and PWK (right), across age groups. Kolmogorov–Smirnov tests were used to evaluate statistical significance (Bonferroni adjusted $p < 0.05$) of pairwise comparisons: young versus middle-aged (YM), middle-aged versus aged (MA), and young versus aged (YA), and p-values reported on each graph (see Table S5). Data points are representative of measures from individual spines. (e) Same as (d) for PFC-to-RE distal tuft spine neck length. Summary statistics for data points represented in each graph reported in Table S5.

resistance to age-related cortical synapse loss. This resistance was evident across both proximal and distal compartments and accompanied by specific forms of spine head and neck remodeling. Decreases in spine neck length should serve to lower the spine neck resistor and effectively increase the efficiency by which current generated at the synapse reaches the parent dendrite. Given the growing links between dendritic mechanisms of integration and the plasticity that mediates learning and memory (Branco & Häusser, 2011; Larkum et al., 2009; Magee, 2000; Spruston, 2008), the putative adaptive spine responses could serve as mechanisms to promote successful maintenance of neuronal health and cognition during aging.

3 | DISCUSSION

Here, we asked whether the effects of aging on synapse number and structure in two specific neural circuits was equivalent across two distinct strains of mice. We chose to investigate B6 and PWK strains as past work has identified them as susceptible or resilient to AD-related cognitive and synaptic deficits, respectively (Gregorová & Forejt, 2000; Heuer et al., 2023; Onos et al., 2019). To rigorously compare across defined neural circuits, we used multisite viral injections to label CA1-to-PFC and PFC-to-RE neurons and systematically sampled ~90,000 spines in proximal and distal dendritic compartments across multiple ages (ranging from 5 to 30 months of age). We found that PFC-projecting CA1 pyramidal cells from both strains maintain their dendritic spine synaptic densities with age, consistent with a body of work examining randomly labeled neurons or synapses in aging NHPs, rats and B6 mice (Buss et al., 2021; Fan et al., 2017; Hof & Morrison, 2004; Morrison & Baxter, 2012; Morrison & Hof, 1997). Conversely, we observed a differential pattern of synapse loss on RE-projecting PFC neurons between B6 and PWK mice, with synapse loss restricted to B6 but not PWK mice. Spine reconstructions suggested that spines from B6 showed either stability or patterns of remodeling putatively associated with decreased synaptic efficacy, whereas PWK spines tended to show morphological changes that are consistent with increased synaptic efficacy during aging (Table S6). These results suggest that previously observed cognitive characteristics from these strains (Onos et al., 2019), including PWK resistance to aging-related decline in cognition or resilience to AD-related neuropathology (Onos et al., 2019) and differential microglia activation (Yang et al., 2021) may be due in part to adaptive forms of synaptic plasticity that maintain connectivity and excitability in cortical circuitry. The PWK mouse strain, then, represents an opportunity to identify and harness adaptive mechanisms to lengthen cognitive resistance to the normal process of aging. This can be tested and validated in future studies, using single synapse functional approaches such as glutamate uncaging (Kasai et al., 2003; Matsuzaki et al., 2004) to evaluate if these structural changes correlate to age-related changes at individual spines in PWK mice.

The viral-based strategy and high-resolution spine reconstructions performed here allowed for specific populations of projection neurons to be compared across mice (Tervo et al., 2016). Past work has relied on disparate techniques, including strategies to label random neurons with dye-filling methods or counting random synapses by EM, to build a coherent picture of synaptic vulnerability of the aging brain (Bloss et al., 2011; Luebke et al., 2004; Ouellette et al., 2020; Peters et al., 2008). By taking advantage of multisite viral strategies to gain projection neuron specificity within the same aging subjects, our results are beginning to identify the neural circuits that are vulnerable to age-related disconnection in terms of information flow. Interplay between CA1 of the hippocampus, PFC and RE is thought to be critical for spatial working memory tasks, a cognitive domain affected in aged individuals (Bizon et al., 2009; Ito et al., 2015; Pliatsikas et al., 2019). Since our most striking finding is the strain-dependent loss on aging PFC-to-RE neurons, our results suggest the PFC may be the critical locus of aging in terms of synapse loss. Reductions in PFC-to-RE spine densities in B6 mice was most dramatic from young to middle-aged, which is consistent with previous findings of synapses on PFC neurons from rats (Bloss et al., 2011, 2013), as well as with behavioral findings that animals and humans start to become impaired in working memory function tasks as early as middle-age (Barnes & McNaughton, 1985; Bizon et al., 2009; Moore et al., 2006; Salthouse, 2009). Although CA1 projection neurons appear to maintain their numbers during aging, our results do not imply that CA1 function is intact during aging. Other processes, including activity-dependent spine plasticity at CA1 synapses, might also contribute to age-related deficits in hippocampal-dependent learning or memory function.

At the level of individual synapses, spine morphology is a strong determinant of function (Kasai et al., 2003; Matsuzaki et al., 2001; Tønnesen et al., 2014). Specifically, spine head diameter is a correlate of synapse strength, spine neck of the level of compartmentalization between the synapse and parent dendrite, and spine type a synthesis of these two parameters into discrete groups. Past work has focused on age-related modification of head diameter with little evidence for modulation of spine neck morphology (Hao et al., 2007). In contrast, our data show that both spine head diameter and neck length are readily modified during aging in a way that depends on genetic context. In B6 mice, CA1-to-PFC neurons exhibited very few morphological spine changes with age, consistent with population stability during aging. Conversely, PWK mice showed consistent evidence for morphological spine remodeling on CA1-to-PFC and PFC-to-RE neurons that suggest an overall increase in efficacy between the spine synapse and parent dendrite (Table S6). When examining spine types, we also observed that CA1-to-PFC neurons from PWK mice reduce long spines (classified as having long necks), while increasing mushroom spines (classified as having large heads) (Figures S1d and S2d). This result did not appear as robust in PFC-to-RE neurons using the categorical spine type approach, probably because PWK mice have ~25% longer spine necks on PFC-to-RE neurons compared to those from B6 (Figure S5). Nevertheless, the shift of spine head diameter and neck length distributions in aging PWK mice across both circuits

examined here are compelling because both spine head and spine neck changes move in unison towards greater synapse efficiency, and their synergism might potentially drive large changes in how excitatory postsynaptic potentials from multiple synapses are integrated in the dendrites.

Recent work from our group has found that female PWK mice are resilient to AD-related synaptic changes in CA1-to-PFC neurons during early exponential phases of pathology spread (Heuer et al., 2023). As biological age is the primary risk factor for developing neurodegenerative disorders including AD (Armstrong, 2019; Launer et al., 1999), the data presented here suggest that the PWK mouse strain can be both a model of resilience to cognitive and synaptic changes seen in AD (Heuer et al., 2023; Onos et al., 2019), and resistance to cortical synapse loss seen during normal brain aging. As in our previous work (Heuer et al., 2023; Yang et al., 2021), only female mice were used in this current study, leaving the role of biological sex on age-related synaptic changes unexamined. Previous reports state that females are more susceptible to age-related neurological disorders such as AD (Podcasy & Epperson, 2016), and female subjects have remained historically underrepresented in scientific research (Bierer et al., 2022). Future work should seek to expand on these results in both male and female mice in experiments powered to detect sex differences.

Since the molecular and cellular mechanisms that differentiate successful from unsuccessful agers are still unknown (Morrison & Hof, 1997), the findings here could drive the identification of cell-specific processes that maintain synapses throughout aging. Future work should seek to advance this goal by testing additional PFC projection neurons to understand the circuit specificity of resistance, by molecular strategies to uncover the gene(s) required for this resistance, and by using functional studies that interrogate how behavior relates to pattens of neuronal activity in these circuits (Göbel & Helmchen, 2007; Kaczorowski et al., 2012). Ultimately, such work would set the stage for developing precise therapeutic strategies to promote healthy cognitive aging and resilience to AD across the genetically diverse and aging human population.

4 | MATERIALS AND METHODS

4.1 | Ethics statement

All research was approved by the Institutional Animal Care and Use Committee (IACUC) at The Jackson Laboratory (approval number 12005 and 20006). Animals were humanely euthanized with 4% tribromoethanol (800 mg/kg). Authors performed their work following guidelines established by "The Eighth Edition of the Guide for the Care and Use of Laboratory Animals" and euthanasia using methods approved by the American Veterinary Medical Association.

4.2 | Animal husbandry

All mice were bred and housed in a 12/12 hour light/dark cycle on aspen bedding and fed a standard 6% Purina 5K52 Chow diet. Experiments were performed using two mouse strains: C57BL/6J (B6, JAX stock #000664) and PWK/PhJ (PWK, JAX stock #003715). Mice were group housed for entirety of experiments. Experimental cohorts were generated through intercrossing B6 or PWK mice to produce 3–8 female mice per age group. Full mouse information is reported in Table S1.

4.3 | Intracranial viral injections

Recombinant adenoassociated viral (AAV) vectors were used to drive Cre-recombinase (AAVretro-Cre) (Tervo et al., 2016), Cre-dependent EGFP (serotype 2/1, AAV-FLEX-*rev*-EGFP) (Graham et al., 2021; Tervo et al., 2016), Flp-recombinase (AAVretro-CAG-FLPo), and FLP-dependent tdTomato (serotype 2/1 AAV-CAG-FRT-*rev*-TdTomato) (Winnubst et al., 2019). AAVretro-CAG-FLPo and AAV-CAG-FRT-*rev*-TdTomato were gifts from Janelia Viral Tools (Addgene plasmid #183412, http://n2t.net/addgene:183412, RRID:Addgene_183,412; Addgene plasmid #191203, http://n2t.net/addgene:191203, RRID:Addgene_191203). The titers of each virus were as follows (in genomic copies/mL): AAVretro-Cre, 1×10^{12}, AAV-FLEX-*rev*-GFP, 1×10^{13}, AAVretro-CAG-FLPo, 1×10^{13}; AAV-CAG-FRT-*rev*-TdTomato, 1×10^{13}. A 1:1 ratio of AAVretro-CAG-FLPo and AAV-FLEX-*rev*-GFP was mixed and 45 nL injected into ventral prefrontal cortex (PFC) over 5 min; 45–50 nL (per each D/V coordinate) of AAV-CAG-FRT-*rev*-TdTomato was injected in CA1 (CA1) over 10 min; AAVretro-Cre was diluted 1:10 with sterile saline and 45 nL injected into nucleus reunions (RE) over 5 min. Since PWK brain volumes are smaller than B6, injection coordinates were adjusted based on pilot experiments to determine injection sites. The coordinates for each injection were as follows (in mm: posterior relative to bregma, lateral relative to midline, and ventral relative to pial surface): B6 PFC (+1.75, −0.95, and −2.6), B6 CA1 (−3.5, −3.4, and − 2.7/−2.5/2.0), B6 RE(−1.1, −1.2, −4.15); PWK PFC (+1.45, −0.9, and − 2.3), PWK CA1 (−3.5, −3.3, and − 2.75/−2.5/−2.0), PWK RE(−1.0, −1.0, −3.2). RE and PFC injections were performed with the mouse tilted at a 15° angle. At each site the injection pipette was left in place for 3–5 min then slowly retracted at a rate of 10 μm/s from the brain. After surgery mice were singly housed, monitored for 5 days, and euthanized approximately 3–4 weeks post injection.

4.4 | Tissue harvest and brain sectioning

Mice were humanely euthanized with an intraperitoneal lethal dose of Tribromoethanol (800 mg/kg), followed by transcardial perfusion with 45 mL ice-cold 4% paraformaldehyde (PFA) in 0.1 M

phosphate-buffered saline, in accordance with IACUC protocols (12,005 and 20,008). Brains were removed and placed in 5 mL ice cold 4% PFA at 4°C for 24 h, then placed into storage buffer (1XPBS + 0.1% Sodium Azide) for long-term storage at 4°C. Brains were coronally sectioned at 50 μm thickness and placed in storage buffer at 4°C until needed for imaging. Approximately six frontal PFC sections containing EGFP+ dendrites, and six sections with distal CA1 TdTomato+ dendrites were mounted on slides and coverslipped using Vectashield Hardset mounting media (Vector Laboratories #H140010).

4.5 | Dendritic spine imaging and analysis

Slices were imaged on a Leica SP8 confocal microscope equipped with a 63× objective (oil immersion), images collected at 50 nm pixel sizes with 0.1 μm z-steps, and stacks deconvolved using Leica Lightning software. Ten dendrites per compartment (e.g., basal, apical oblique, tuft) were captured per mouse. Each image was exported as TIFF format (in ImageJ version 2.9.0/1.53t) and imported into NeuronStudio (Rodriguez et al., 2008) for analysis of dendritic spine densities and morphologies. Since the effectiveness of a synaptic input on the dendritic tree is influenced by the diameter of the parent dendrite (Holmes, 1989), we ensured all dendritic calibers incorporated into this analysis were thin (i.e. under 1 μm in diameter) (Figures S1a, S2a, S3a, S4a). Density measurements were acquired by first reconstructing the dendritic cable followed by semi-automated spine identification. Cumulative distributions of assigned spine head diameters (HEAD.DIAMETER) and neck lengths (MAX.DTS) were analyzed by Kolmogorov–Smirnov tests, and through a quartile-based analysis. In this latter analysis, spines within dendritic compartments from each strain were pooled across treatment groups to create a population, and the first and last quartiles determined. From each branch, spines belonging to the first quartile (Q1, smallest) and last quartile (Q4, largest) were identified and the density for each quartile per branch was calculated. Data were analyzed with each dendrite representing an individual data point.

4.6 | Spine type classifications

Dendritic spines were morphologically classified into one of four categories based on previously established criteria (Dumitriu et al., 2010; Risher et al., 2014): Long, Thin, Mushroom, and Stubby. Long spines were classified by any spine with a neck length (MAX.DTS) greater than 1 μm. Mushroom spines were classified as any spine with a neck length less than 1 μm and head diameter (HEAD.DIAMETER) greater than 0.3 μm. Thin spines were classified as any spine with a neck length between 0.3 μm and 1 μm, and head diameter less than 0.3 μm. Stubby spines were classified as any spine with a neck length and head diameter less than 0.3 μm. Once spines were morphologically classified, the percentage of each spine type was calculated for each analyzed dendrite, and data analyzed as each dendrite representing an individual data point.

4.7 | Statistical analysis

Data were analyzed blinded to strain and age group. All statistical analyses were performed in GraphPad Prism software (v9.5.1) except for Kolmogorov–Smirnov (K-S) tests which were performed using R (v4.2.2). Results are reported in table form in the Supplemental Information (Table S2-S5). Data from B6 and PWK mouse strains were analyzed separately. To assess age effects within each strain, one-way ANOVAs were computed followed by Bonferroni post hoc tests. Within-group differences between Q1 and Q4 densities for spine head diameter and neck length were determined using non-parametric two-tailed t tests. Bonferroni corrections for multiple comparisons were performed on nominal *p*-values from resultant K–S tests.

AUTHOR CONTRIBUTIONS

Sarah E. Heuer, Erik B. Bloss, and Gareth R. Howell designed the study. Sarah E. Heuer generated and maintained mouse cohorts, and Sarah E. Heuer and Erik B. Bloss performed the intracranial AAV injections. Sarah E. Heuer euthanized mice and collected tissues. Sarah E. Heuer and Emily W. Nickerson sectioned brains and prepared slides for imaging. Sarah E. Heuer and Emily W. Nickerson imaged slices and analyzed final data. Erik B. Bloss provided training in intracranial injections, confocal microscopy imaging of dendrites and dendritic spines, and NeuronStudio analysis. Erik B. Bloss and Gareth R. Howell advised on all data analysis, data interpretation and manuscript preparation. Sarah E. Heuer, Emily W. Nickerson, Erik B. Bloss and Gareth R. Howell wrote and edited the manuscript. All authors approved the final version.

ACKNOWLEDGEMENTS

We thank Dr. Kristen Onos and Kelly Keezer for providing aged PWK/PhJ mouse cohorts, and Amanda Hewes and Melanie-Maddox Goodrich for providing critical laboratory support for the initiation of these experiments. We also thank Dr. Philipp Henrich at the Microscopy core at The Jackson Laboratory for training and assistance on the confocal microscope.

FUNDING INFORMATION

This study was supported by the National Institute on Aging (NIA) AG079877 (E.B.B.), AG055104 (G.R.H.), program funds from The Jackson Laboratory (G.R.H.), and by the NIA T32 training program AG062409 in the Precision Genetics of Aging, Alzheimer's Disease and Related Dementias at The Jackson Laboratory (S.E.H., G.R.H., E.B.B.). Authors are extremely grateful for the support of the Diana Davis Spencer Foundation.

CONFLICT OF INTEREST STATEMENT

The authors have no conflicts or competing interests to declare.

DATA AVAILABILITY STATEMENT

All mouse strains are available through The Jackson Laboratory. All reagents in this study are commercially available. Raw data (DOI: 10.6084/m9.figshare.23620752) and images from the figures (DOI: 10.6084/m9.figshare.23620755) are available via Figshare (made public upon acceptance of publication).

PERMISSION STATEMENT

We permit the right to Wiley and *Aging Cell* to license and reproduce the above information. We required no permissions for any data or figures produced in this manuscript.

ORCID

Sarah E. Heuer https://orcid.org/0000-0003-4461-2386
Emily W. Nickerson https://orcid.org/0000-0002-0397-6514
Gareth R. Howell https://orcid.org/0000-0003-0565-6474
Erik B. Bloss https://orcid.org/0000-0001-5031-4591

REFERENCES

Araya, R., Jiang, J., Eisenthal, K. B., & Yuste, R. (2006). The spine neck filters membrane potentials. *Proceedings of the National Academy of Sciences*, *103*, 17961–17966.

Armstrong, R. A. (2019). Risk factors for Alzheimer's disease. *Folia Neuropathologica*, *57*, 87–105.

Bailey, M. E., Wang, A. C. J., Hao, J., Janssen, W. G. M., Hara, Y., Dumitriu, D., Hof, P. R., & Morrison, J. H. (2011). Interactive effects of age and estrogen on cortical neurons: Implications for cognitive aging. *Neuroscience*, *191*, 148–158.

Barnes, C. A., & McNaughton, B. L. (1985). An age comparison of the rates of acquisition and forgetting of spatial information in relation to long-term enhancement of hippocampal synapses. *Behavioral Neuroscience*, *99*, 1040–1048.

Baxter, M. G., Santistevan, A. C., Bliss-Moreau, E., & Morrison, J. H. (2018). Timing of cyclic estradiol treatment differentially affects cognition in aged female rhesus monkeys. *Behavioral Neuroscience*, *132*, 213–223.

Bayer, H., & Bertoglio, L. J. (2020). Infralimbic cortex controls fear memory generalization and susceptibility to extinction during consolidation. *Scientific Reports*, *10*, 15827.

Bierer, B. E., Meloney, L. G., Ahmed, H. R., & White, S. A. (2022). Advancing the inclusion of underrepresented women in clinical research. *Cell reports. Medicine*, *3*(4), 100553.

Bizon, J. L., LaSarge, C. L., Montgomery, K. S., McDermott, A. N., Setlow, B., & Griffith, W. H. (2009). Spatial reference and working memory across the lifespan of male Fischer 344 rats. *Neurobiology of Aging*, *30*, 646–655.

Blanpied, T. A., & Ehlers, M. D. (2004). Microanatomy of dendritic spines: Emerging principles of synaptic pathology in psychiatric and neurological disease. *Biological Psychiatry*, *55*, 1121–1127.

Bloss, E. B., Cembrowski, M. S., Karsh, B., Colonell, J., Fetter, R. D., & Spruston, N. (2016). Structured dendritic inhibition supports branch-selective integration in CA1 pyramidal cells. *Neuron*, *89*, 1016–1030.

Bloss, E. B., Cembrowski, M. S., Karsh, B., Colonell, J., Fetter, R. D., & Spruston, N. (2018). Single excitatory axons form clustered synapses onto CA1 pyramidal cell dendrites. *Nature Neuroscience*, *21*, 353–363.

Bloss, E. B., Janssen, W. G., Ohm, D. T., Yuk, F. J., Wadsworth, S., Saardi, K. M., McEwen, B. S., & Morrison, J. H. (2011). Evidence for reduced experience-dependent dendritic spine plasticity in the aging prefrontal cortex. *The Journal of Neuroscience*, *31*, 7831–7839.

Bloss, E. B., Puri, R., Yuk, F., Punsoni, M., Hara, Y., Janssen, W. G., McEwen, B. S., & Morrison, J. H. (2013). Morphological and molecular changes in aging rat prelimbic prefrontal cortical synapses. *Neurobiology of Aging*, *34*, 200–210.

Branco, T., & Häusser, M. (2011). Synaptic integration gradients in single cortical pyramidal cell dendrites. *Neuron*, *69*, 885–892.

Brennan, A. R., Yuan, P., Dickstein, D. L., Rocher, A. B., Hof, P. R., Manji, H., & Arnsten, A. F. T. (2009). Protein kinase C activity is associated with prefrontal cortical decline in aging. *Neurobiology of Aging*, *30*, 782–792.

Brown, S. P., & Hestrin, S. (2009). Intracortical circuits of pyramidal neurons reflect their long-range axonal targets. *Nature*, *457*, 1133–1136.

Burke, S. N., & Barnes, C. A. (2006). Neural plasticity in the ageing brain. *Nature Reviews. Neuroscience*, *7*, 30–40.

Buss, E. W., Corbett, N. J., Roberts, J. G., Ybarra, N., Musial, T. F., Simkin, D., Molina-Campos, E., Oh, K.-J., Nielsen, L. L., Ayala, G. D., Mullen, S. A., Farooqi, A. K., D'Souza, G. X., Hill, C. L., Bean, L. A., Rogalsky, A. E., Russo, M. L., Curlik, D. M., Antion, M. D., … Nicholson, D. A. (2021). Cognitive aging is associated with redistribution of synaptic weights in the hippocampus. *Proceedings of the National Academy of Sciences*, *118*, e1921481118.

Cajal, S. R. (1888). Estructura de los centros nerviosos de las aves. *Revista trimestral de histología normal y patológica*, *1*, 1.

Cizeron, M., Qiu, Z., Koniaris, B., Gokhale, R., Komiyama, N. H., Fransén, E., & Grant, S. G. N. (2020). A brainwide atlas of synapses across the mouse life span. *Science*, *369*, 270–275.

Dickstein, D. L., Weaver, C. M., Luebke, J. I., & Hof, P. R. (2013). Dendritic spine changes associated with normal aging. *Neuroscience*, *251*, 21–32.

Druckmann, S., Feng, L., Lee, B., Yook, C., Zhao, T., Magee, J. C., & Kim, J. (2014). Structured synaptic connectivity between hippocampal regions. *Neuron*, *81*, 629–640.

Dumitriu, D., Hao, J., Hara, Y., Kaufmann, J., Janssen, W. G. M., Lou, W., Rapp, P. R., & Morrison, J. H. (2010). Selective changes in thin spine density and morphology in monkey prefrontal cortex correlate with aging-related cognitive impairment. *The Journal of Neuroscience*, *30*, 7507–7515.

Empson, R. M., & Heinemann, U. (1995). The perforant path projection to hippocampal area CA1 in the rat hippocampal-entorhinal cortex combined slice. *The Journal of Physiology*, *484*, 707–720.

Fan, X., Wheatley, E. G., & Villeda, S. A. (2017). Mechanisms of hippocampal aging and the potential for rejuvenation. *Annual Review of Neuroscience*, *40*, 251–272.

Fernandes, C., Liu, L., Paya-Cano, J. L., Gregorová, S., Forejt, J., & Schalkwyk, L. C. (2004). Behavioral characterization of wild derived male mice (Mus musculus musculus) of the PWD/Ph inbred strain: High exploration compared to C57BL/6J. *Behavior Genetics*, *34*, 621–630.

Geinisman, Y., Ganeshina, O., Yoshida, R., Berry, R. W., Disterhoft, J. F., & Gallagher, M. (2004). Aging, spatial learning, and total synapse number in the rat CA1 stratum radiatum. *Neurobiology of Aging*, *25*, 407–416.

Ghani, M. U., Mesadi, F., Kanık, S. D., Argunşah, A. Ö., Hobbiss, A. F., Israely, I., Ünay, D., Taşdizen, T., & Çetin, M. (2017). Dendritic spine classification using shape and appearance features based on two-photon microscopy. *Journal of Neuroscience Methods*, *279*, 13–21.

Gidon, A., & Segev, I. (2012). Principles governing the operation of synaptic inhibition in dendrites. *Neuron*, *75*, 330–341.

Göbel, W., & Helmchen, F. (2007). In vivo calcium imaging of neural network function. *Physiology*, *22*, 358–365.

Graham, K., Spruston, N., & Bloss, E. B. (2021). Hippocampal and thalamic afferents form distinct synaptic microcircuits in the mouse infralimbic frontal cortex. *Cell Reports*, *37*, 109837.

Gregorová, S., & Forejt, J. (2000). PWD/Ph and PWK/Ph inbred mouse strains of Mus m. musculus subspecies–a valuable resource of phenotypic variations and genomic polymorphisms. *Folia Biologica*, *46*, 31–41.

Grunditz, Å., Holbro, N., Tian, L., Zuo, Y., & Oertner, T. G. (2008). Spine neck plasticity controls postsynaptic calcium signals through electrical compartmentalization. *The Journal of Neuroscience*, *28*, 13457–13466.

Hampel, H., Hardy, J., Blennow, K., Chen, C., Perry, G., Kim, S. H., Villemagne, V. L., Aisen, P., Vendruscolo, M., Iwatsubo, T., Masters, C. L., Cho, M., Lannfelt, L., Cummings, J. L., & Vergallo, A. (2021). The amyloid-β pathway in Alzheimer's disease. *Molecular Psychiatry*, *26*, 5481–5503.

Hao, J., Rapp, P. R., Janssen, W. G. M., Lou, W., Lasley, B. L., Hof, P. R., & Morrison, J. H. (2007). Interactive effects of age and estrogen on cognition and pyramidal neurons in monkey prefrontal cortex. *Proceedings of the National Academy of Sciences of the United States of America*, *104*, 11465–11470.

Hara, Y., Rapp, P. R., & Morrison, J. H. (2012). Neuronal and morphological bases of cognitive decline in aged rhesus monkeys. *Age*, *34*, 1051–1073.

Harvey, C. D., & Svoboda, K. (2007). Locally dynamic synaptic learning rules in pyramidal neuron dendrites. *Nature*, *450*, 1195–1200.

Hering, H., & Sheng, M. (2001). Dentritic spines: Structure, dynamics and regulation. *Nature Reviews. Neuroscience*, *2*, 880–888.

Heuer, S. E., Keezer, K. J., Hewes, A. A., Onos, K. D., Graham, K. C., Howell, G. R., & Bloss, E. B. (2023). Control of hippocampal synaptic plasticity by microglia-dendrite interactions depends on genetic context in mouse models of Alzheimer's disease. *Alzheimer's & dementia*. https://doi.org/10.1002/alz.13440 [Online ahead of print].

Hof, P. R., & Morrison, J. H. (2004). The aging brain: Morphomolecular senescence of cortical circuits. *Trends in Neurosciences*, *27*, 607–613.

Holmes, W. R. (1989). The role of dendritic diameters in maximizing the effectiveness of synaptic inputs. *Brain Research*, *478*, 127–137.

Ito, H. T., Zhang, S.-J., Witter, M. P., Moser, E. I., & Moser, M.-B. (2015). A prefrontal-thalamo-hippocampal circuit for goal-directed spatial navigation. *Nature*, *522*, 50–55.

Jacobsen, J. S., Wu, C.-C., Redwine, J. M., Comery, T. A., Arias, R., Bowlby, M., Martone, R., Morrison, J. H., Pangalos, M. N., Reinhart, P. H., & Bloom, F. E. (2006). Early-onset behavioral and synaptic deficits in a mouse model of Alzheimer's disease. *Proceedings of the National Academy of Sciences of the United States of America*, *103*, 5161–5166.

Kaczorowski, C. C., Davis, S. J., & Moyer, J. R. (2012). Aging redistributes medial prefrontal neuronal excitability and impedes extinction of trace fear conditioning. *Neurobiology of Aging*, *33*, 1744–1757.

Kasai, H., Matsuzaki, M., Noguchi, J., Yasumatsu, N., & Nakahara, H. (2003). Structure–stability–function relationships of dendritic spines. *Trends in Neurosciences*, *26*, 360–368.

Katz, Y., Menon, V., Nicholson, D. A., Geinisman, Y., Kath, W. L., & Spruston, N. (2009). Synapse distribution suggests a two-stage model of dendritic integration in CA1 pyramidal neurons. *Neuron*, *63*, 171–177.

Kaufman, S. K., Del Tredici, K., Thomas, T. L., Braak, H., & Diamond, M. I. (2018). Tau seeding activity begins in the transentorhinal/entorhinal regions and anticipates phospho-tau pathology in Alzheimer's disease and PART. *Acta Neuropathologica*, *136*, 57–67.

Keane, T. M., Goodstadt, L., Danecek, P., White, M. A., Wong, K., Yalcin, B., Heger, A., Agam, A., Slater, G., Goodson, M., Furlotte, N. A., Eskin, E., Nellåker, C., Whitley, H., Cleak, J., Janowitz, D., Hernandez-Pliego, P., Edwards, A., Belgard, T. G., … Adams, D. J. (2011). Mouse genomic variation and its effect on phenotypes and gene regulation. *Nature*, *477*, 289–294.

Koch, C., Poggio, T., & Torre, V. (1983). Nonlinear interactions in a dendritic tree: Localization, timing, and role in information processing. *Proceedings of the National Academy of Sciences of the United States of America*, *80*, 2799–2802.

Larkum, M. E., Nevian, T., Sandler, M., Polsky, A., & Schiller, J. (2009). Synaptic integration in tuft dendrites of layer 5 pyramidal neurons: A new unifying principle. *Science*, *325*, 756–760.

Launer, L. J., Andersen, K., Dewey, M. E., Letenneur, L., Ott, A., Amaducci, L. A., Brayne, C., Copeland, J. R., Dartigues, J. F., Kragh-Sorensen, P., Lobo, A., Martinez-Lage, J. M., Stijnen, T., & Hofman, A. (1999). Rates and risk factors for dementia and Alzheimer's disease: Results from EURODEM pooled analyses. EURODEM incidence research group and work groups. European studies of dementia. *Neurology*, *52*, 78–84.

Lerner, T. N., Ye, L., & Deisseroth, K. (2016). Communication in neural circuits: Tools, opportunities, and challenges. *Cell*, *164*, 1136–1150.

Luebke, J. I., Chang, Y.-M., Moore, T. L., & Rosene, D. L. (2004). Normal aging results in decreased synaptic excitation and increased synaptic inhibition of layer 2/3 pyramidal cells in the monkey prefrontal cortex. *Neuroscience*, *125*, 277–288.

Magee, J. C. (2000). Dendritic integration of excitatory synaptic input. *Nature Reviews. Neuroscience*, *1*, 181–190.

Matsuzaki, M., Ellis-Davies, G. C., Nemoto, T., Miyashita, Y., Iino, M., & Kasai, H. (2001). Dendritic spine geometry is critical for AMPA receptor expression in hippocampal CA1 pyramidal neurons. *Nature Neuroscience*, *4*, 1086–1092.

Matsuzaki, M., Honkura, N., Ellis-Davies, G. C. R., & Kasai, H. (2004). Structural basis of long-term potentiation in single dendritic spines. *Nature*, *429*, 761–766.

Megías, M., Emri, Z., Freund, T. F., & Gulyás, A. I. (2001). Total number and distribution of inhibitory and excitatory synapses on hippocampal CA1 pyramidal cells. *Neuroscience*, *102*, 527–540.

Moore, T. L., Killiany, R. J., Herndon, J. G., Rosene, D. L., & Moss, M. B. (2006). Executive system dysfunction occurs as early as middle-age in the rhesus monkey. *Neurobiology of Aging*, *27*, 1484–1493.

Morrison, J. H., & Baxter, M. G. (2012). The ageing cortical synapse: Hallmarks and implications for cognitive decline. *Nature Reviews. Neuroscience*, *13*, 240–250.

Morrison, J. H., & Hof, P. R. (1997). Life and death of neurons in the aging brain. *Science*, *278*, 412–419.

Moss, M. B., Moore, T. L., Schettler, S. P., Killiany, R., & Rosene, D. (2007). Successful vs. unsuccessful aging in the rhesus monkey. In D. R. Riddle (Ed.), *Brain aging: Models, methods, and mechanisms*. *Frontiers in neuroscience*. CRC Press/Taylor & Francis.

Neuman, K. M., Molina-Campos, E., Musial, T. F., Price, A. L., Oh, K.-J., Wolke, M. L., Buss, E. W., Scheff, S. W., Mufson, E. J., & Nicholson, D. A. (2015). Evidence for Alzheimer's disease-linked synapse loss and compensation in mouse and human hippocampal CA1 pyramidal neurons. *Brain Structure & Function*, *220*, 3143–3165.

Nicholson, D. A., Yoshida, R., Berry, R. W., Gallagher, M., & Geinisman, Y. (2004). Reduction in size of perforated postsynaptic densities in hippocampal axospinous synapses and age-related spatial learning impairments. *Journal of Neuroscience: The Official Journal of the Society for Neuroscience*, *24*, 7648–7653.

Onos, K. D., Uyar, A., Keezer, K. J., Jackson, H. M., Preuss, C., Acklin, C. J., O'Rourke, R., Buchanan, R., Cossette, T. L., Sukoff Rizzo, S. J., Soto, I., Carter, G. W., & Howell, G. R. (2019). Enhancing face validity of mouse models of Alzheimer's disease with natural genetic variation. *PLoS Genetics*, *15*, e1008155.

Ouellette, A. R., Neuner, S. M., Dumitrescu, L., Anderson, L. C., Gatti, D. M., Mahoney, E. R., Bubier, J. A., Churchill, G., Peters, L., Huentelman, M. J., Herskowitz, J. H., Yang, H.-S., Smith, A. N., Reitz, C., Kunkle, B. W., White, C. C., De Jager, P. L., Schneider, J. A., Bennett, D. A., … Kaczorowski, C. C. (2020). Cross-species analyses identify Dlgap2 as a regulator of age-related cognitive decline and Alzheimer's dementia. *Cell Reports*, *32*, 108091.

Petanjek, Z., Judaš, M., Šimić, G., Rašin, M. R., Uylings, H. B. M., Rakic, P., & Kostović, I. (2011). Extraordinary neoteny of synaptic spines in the human prefrontal cortex. *Proceedings of the National Academy of Sciences*, *108*, 13281–13286.

Peters, A., Sethares, C., & Luebke, J. I. (2008). Synapses are lost during aging in the primate prefrontal cortex. *Neuroscience*, *152*, 970–981.

Pliatsikas, C., Veríssimo, J., Babcock, L., Pullman, M. Y., Glei, D. A., Weinstein, M., Goldman, N., & Ullman, M. T. (2019). Working memory in older adults declines with age, but is modulated by sex and education. *The Quarterly Journal of Experimental Psychology 2006*, *72*, 1308–1327.

Podcasy, J. L., & Epperson, C. N. (2016). Considering sex and gender in Alzheimer disease and other dementias. *Dialogues in Clinical Neuroscience*, *18*, 437–446.

Rasmussen, T., Schliemann, T., Sørensen, J. C., Zimmer, J., & West, M. J. (1996). Memory impaired aged rats: no loss of principal hippocampal and subicular neurons. *Neurobiology of Aging*, *17*, 143–147.

Risher, W. C., Ustunkaya, T., Alvarado, J. S., & Eroglu, C. (2014). Rapid golgi analysis method for efficient and unbiased classification of dendritic spines. *PLoS One*, *9*, e107591.

Rodriguez, A., Ehlenberger, D. B., Dickstein, D. L., Hof, P. R., & Wearne, S. L. (2008). Automated three-dimensional detection and shape classification of dendritic spines from fluorescence microscopy images. *PLoS One*, *3*, e1997.

Runge, K., Cardoso, C., & de Chevigny, A. (2020). Dendritic spine plasticity: Function and mechanisms. *Frontiers in Synaptic Neuroscience*, *12*, 36.

Salthouse, T. A. (2009). When does age-related cognitive decline begin? *Neurobiology of Aging*, *30*, 507–514.

Scheff, S. W., Price, D. A., & Sparks, D. L. (2001). Quantitative assessment of possible age-related change in synaptic numbers in the human frontal cortex. *Neurobiology of Aging*, *22*, 355–365.

Scheff, S. W., Scott, S. A., & DeKosky, S. T. (1991). Quantitation of synaptic density in the septal nuclei of young and aged Fischer 344 rats. *Neurobiology of Aging*, *12*, 3–12.

Serrano, M. E., Kim, E., Petrinovic, M. M., Turkheimer, F., & Cash, D. (2022). Imaging synaptic density: The next holy grail of neuroscience? *Frontiers in Neuroscience*, *16*, 796129.

Shimada, A., Keino, H., Satoh, M., Kishikawa, M., & Hosokawa, M. (2003). Age-related loss of synapses in the frontal cortex of SAMP10 mouse: A model of cerebral degeneration. *Synapse*, *48*, 198–204.

Sorra, K. E., & Harris, K. M. (2000). Overview on the structure, composition, function, development, and plasticity of hippocampal dendritic spines. *Hippocampus*, *10*, 501–511.

Spruston, N. (2008). Pyramidal neurons: Dendritic structure and synaptic integration. *Nature Reviews. Neuroscience*, *9*, 206–221.

Südhof, T. C., & Malenka, R. C. (2008). Understanding synapses: Past, present, and future. *Neuron*, *60*, 469–476.

Tervo, D. G. R., Hwang, B.-Y., Viswanathan, S., Gaj, T., Lavzin, M., Ritola, K. D., Lindo, S., Michael, S., Kuleshova, E., Ojala, D., Huang, C.-C., Gerfen, C. R., Schiller, J., Dudman, J. T., Hantman, A. W., Looger, L. L., Schaffer, D. V., & Karpova, A. Y. (2016). A designer AAV variant permits efficient retrograde access to projection neurons. *Neuron*, *92*, 372–382.

Tønnesen, J., Katona, G., Rózsa, B., & Nägerl, U. V. (2014). Spine neck plasticity regulates compartmentalization of synapses. *Nature Neuroscience*, *17*, 678–685.

Turrigiano, G. (2012). Homeostatic synaptic plasticity: Local and global mechanisms for stabilizing neuronal function. *Cold Spring Harbor Perspectives in Biology*, *4*, a005736.

Turrigiano, G. G. (2008). The self-tuning neuron: Synaptic scaling of excitatory synapses. *Cell*, *135*, 422–435.

Villeda, S. A., Plambeck, K. E., Middeldorp, J., Castellano, J. M., Mosher, K. I., Luo, J., Smith, L. K., Bieri, G., Lin, K., Berdnik, D., Wabl, R., Udeochu, J., Wheatley, E. G., Zou, B., Simmons, D. A., Xie, X. S., Longo, F. M., & Wyss-Coray, T. (2014). Young blood reverses age-related impairments in cognitive function and synaptic plasticity in mice. *Nature Medicine*, *20*, 659–663.

Wang, M., Ramos, B. P., Paspalas, C. D., Shu, Y., Simen, A., Duque, A., Vijayraghavan, S., Brennan, A., Dudley, A., Nou, E., Mazer, J. A., McCormick, D. A., & Arnsten, A. F. T. (2007). Alpha2A-adrenoceptors strengthen working memory networks by inhibiting cAMP-HCN channel signaling in prefrontal cortex. *Cell*, *129*, 397–410.

Winnubst, J., Bas, E., Ferreira, T. A., Wu, Z., Economo, M. N., Edson, P., Arthur, B. J., Bruns, C., Rokicki, K., Schauder, D., Olbris, D. J., Murphy, S. D., Ackerman, D. G., Arshadi, C., Baldwin, P., Blake, R., Elsayed, A., Hasan, M., Ramirez, D., … Chandrashekar, J. (2019). Reconstruction of 1,000 projection neurons reveals new cell types and organization of long-range connectivity in the mouse brain. *Cell*, *179*, 268–281.e13.

Yang, H. S., Onos, K. D., Choi, K., Keezer, K. J., Skelly, D. A., Carter, G. W., & Howell, G. R. (2021). Natural genetic variation determines microglia heterogeneity in wild-derived mouse models of Alzheimer's disease. *Cell Reports*, *34*(6), 108739.

Young, M. E., Ohm, D. T., Dumitriu, D., Rapp, P. R., & Morrison, J. H. (2014). Differential effects of aging on dendritic spines in visual cortex and prefrontal cortex of the rhesus monkey. *Neuroscience*, *274*, 33–43.

SUPPORTING INFORMATION

Additional supporting information can be found online in the Supporting Information section at the end of this article.

How to cite this article: Heuer, S. E., Nickerson, E. W., Howell, G. R., & Bloss, E. B. (2024). Genetic context drives age-related disparities in synaptic maintenance and structure across cortical and hippocampal neuronal circuits. *Aging Cell*, *23*, e14033. https://doi.org/10.1111/acel.14033